

Optical Waveguiding and Morphology of Chitosan Thin Films

HAO JIANG,^{1,*} W. SU,² S. CARACCI,² T. J. BUNNING,³ T. COOPER,² and W. W. ADAMS²

¹Ogden Professional Services/Lawrence Associates, Inc., 5100 Springfield Pike, Suite 509, Dayton, Ohio 45431;

²Materials Directorate, Wright Laboratory, WPAFB, Ohio 45433-7702; ³Science Applications International Corporation, 101 Woodman Dr., Dayton, Ohio 45431

SYNOPSIS

An investigation was made of the optical and waveguiding properties of thin films fabricated from solutions of chitosan-acetic acid (chitosan/HAc) and chitosan/HAc doped with rare-earth metal ions (Er^{+++} or Nd^{+++}). For all three films, the refractive indices were approximately 1.5 and there was nearly no absorption in the range of 300 to 2700 nm. The optical loss in a waveguides was less than 0.5 dB/cm. Morphological observations disclosed that all the films possessed a dense and homogeneous amorphous structure with smooth surfaces. Extrinsic scattering, especially the scattering caused by surface impurities, was the dominating factor affecting the optical loss value. It is also interesting to note that for all the films, doped with rare-earth metal ions or not, the morphological characteristics were alike and the optical properties were similar. Doping rare-earth metal ions into chitosan thin films did not seriously influence optical waveguiding. This paper reports, we believe, the first study of chitosan films for optical applications. The experimental results demonstrate that chitosan and its derivatives are potential candidates for optical materials. © 1996 John Wiley & Sons, Inc.

INTRODUCTION

In the past 10 years, research has dramatically increased on organic and polymeric materials as promising candidate media for optical information transmission, storage, and processing. This interest has arisen from advantages that polymers possess, including good optical and mechanical properties, high structural integrity, excellent processability, and inexpensive raw material costs.^{1,2} Furthermore, polymers have achieved fundamental success in improving desired structures and properties by molecular design. In recent years, polymers have increasingly been studied as possible waveguide materials. Polymeric materials have exhibited relatively low optical loss at the important communication wavelengths of 830 nm, 1.3 μm , and 1.5 μm , processing compatibility with microelectronic and optical devices, and a wide variety of special properties in-

cluding refractive index tailoring. Barriers still exist to produce successful materials with the combined attributes of low propagation loss, high temperature stability, and excellent electronic packaging process capability.³⁻⁶ It is also interesting to note that rare-earth ions such as erbium and neodymium, when doped into the right glass or matrix, can be used to build optical amplifiers or lasers with optical pumping.⁷ During the past 10 years, intense research on single-mode rare-earth-doped fiber lasers and amplifiers has led to rapid growth of a series of active devices.⁸⁻¹⁰ It has also been reported recently that the chemical compounds containing rare-earth metal ions (REMI) can be successfully mixed with host polymer materials to produce REMI-doped polymer waveguide amplifiers.¹¹

Chitosan is an interesting polysaccharide, which can be easily derived from chitin by *N*-deacetylation. Chitin is widely found in nature as a major component of the cell wall of various fungi and in the shells of insects and crustaceans. Figure 1 shows the molecular repeat units of chitosan, containing β -1-4-linked 2-amino-2-deoxy-D-glucopyranose, and

* To whom correspondence should be addressed.

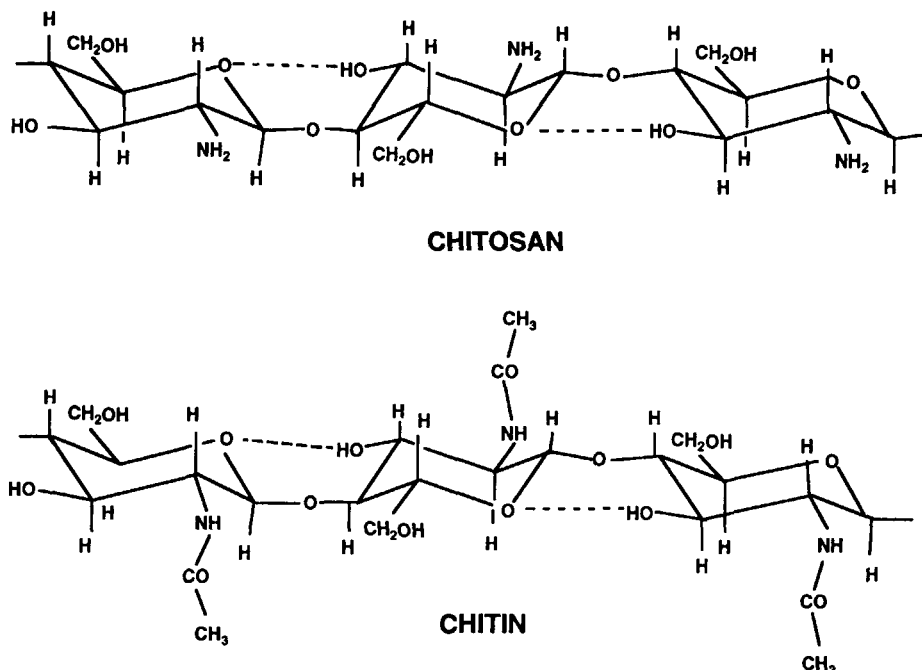


Figure 1 Molecular structures of chitin and chitosan.

chitin, poly-*N*-acetyl-D-glucosamine. In the recent decade, chitosan has received much attention for its special properties and inexpensive, abundant resources. Research has not only concentrated in traditional areas such as waste water treatment and medical fibers and films, but also for potential applications in many other areas including industry, agriculture, food, and biology.¹²⁻¹⁴ Recently, our laboratory has achieved progress in applying chitosan for optics applications. In the present article, we describe the processing conditions and characterization of chitosan thin film fabricated from chitosan/acetic acid (HAc) solutions as optical waveguiding materials. Based on the high affinities of chitosan for metal ions, films of chitosan doped with rare-earth metal ions have also been studied for their optical waveguiding properties.

EXPERIMENTAL

Materials and Processing

The chitosan used for making thin films was supplied by Fluka with either low molecular weight (MW: about 70,000) or medium molecular weight (MW: about 750,000). Chitosan was dissolved in an HAc aqueous solution (0.5–10 wt %) to form the precursor solution with 0.5–5 wt % chitosan. The rare-earth metal ions, used to dope the chitosan solutions, were Nd^{3+} [$\text{Nd}(\text{NO}_3)_3$] and Er^{3+} (ErCl_3).

Doping ratios around 5–50 wt % relative to chitosan were used.

All solutions were filtered carefully through a glass sinter filter (medium grade). Films were prepared for characterization by spin-coating (with spinning rates of 30–250 rpm) or casting the precursor solutions on silicon, $\text{SiO}_2/\text{silicon}$, quartz, glass, or polyethylene substrates at room temperature. The films were immediately dried in a vacuum chamber at 55°C for 4 h. The thickness of the prepared films ranged from 0.3 to 10 microns as measured by a Dektak IIA surface profiling system (Sloan Technology Co.) and spectroscopic ellipsometry (Rudolph Instruments S2000).

Waveguiding Measurement

Optical waveguide loss measurements on chitosan films were performed using the out-of-plane scattering technique at 830 nm.¹⁵ Shown schematically

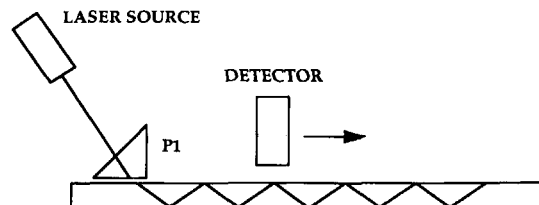


Figure 2 A schematic of the out-of-plane loss measurement technique (see Ref. 15).

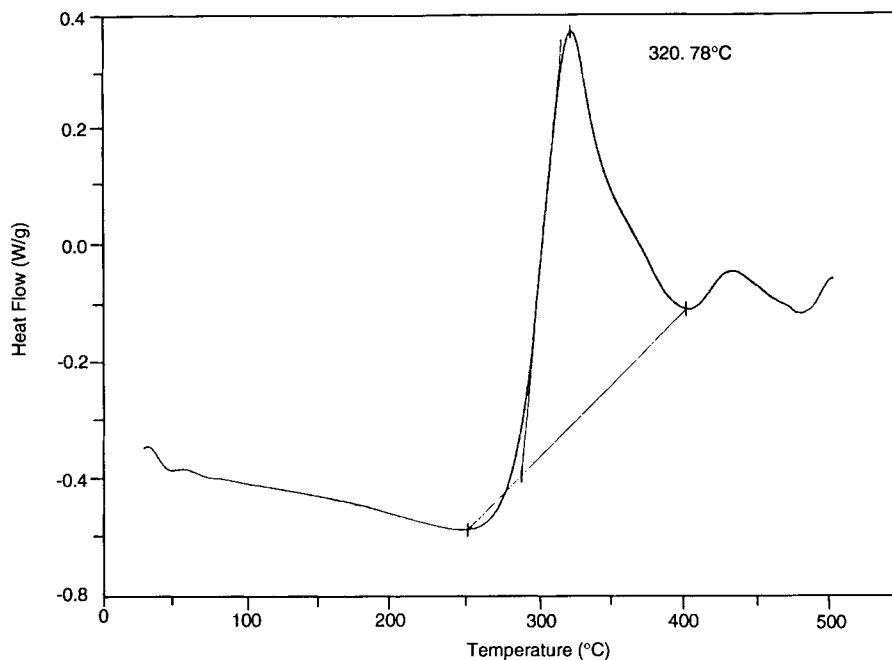


Figure 3 A DSC spectra of chitosan obtained under N_2 at a heating rate of $20^\circ\text{C}/\text{min}$ showing a large decomposition peak above 300°C .

in Figure 2 is a diagram of the experimental setup for this measurement technique. Light was coupled into the waveguide via a rutile prism. A large area silicon detector was used to measure the light scattered perpendicular to the waveguide film as the detector was moved along the waveguide. Generally, silicon wafers (76 and 51 mm diameter) with a 2 micron-thick layer of thermally grown silica (SiO_2) were used as substrates for the waveguide measurements. The typical waveguide lengths were about 3–6 cm. To obtain reliable results, several measurements across the wafer were selected to obtain an average loss value. (Normally, at least three positions were chosen for each tested film.) Assuming that there is a uniform distribution of scattering centers in the waveguide, the loss is calculated from a fit to the measured data according to Beer's Law,

$$I = I_0 e^{-\alpha z}$$

where I_0 is the input intensity; α , the loss coefficient; and z , the distance of propagation. Therefore, the loss (dB/cm) = $(\alpha/z)\log(I_0/I)$, where a is a logarithmic conversion constant.¹⁶

Film Characterization

The thermal properties of the films were measured by a differential scanning calorimeter (DSC) (TA

Instruments DSC2920). The refractive indices and optical absorption of the films were determined by spectroscopic ellipsometry in the reflectance mode and standard UV-vis spectrometry (Perkin-Elmer $\lambda 9$) in the transmission mode. The morphology of the films was probed with a transmission electron microscope (TEM, JEOL 100CX), a low-voltage high-resolution scanning electron microscope (LVHRSEM, Hitachi S900), an atomic force microscope (Park Scientific Instruments SFM BD2), and a rotating anode X-ray generator (Rigaku RU300) with a Statton camera. For LVHRSEM measurements, film samples were coated with 10–20 Å tungsten using a dual-ion beam coater to eliminate charging and increase contrast.

RESULTS AND DISCUSSION

By considering the thermal behavior of chitosan films as a function of temperature, it is possible to obtain information about their thermal stability. Figure 3 is a DSC diagram of chitosan. The heating rate was $20^\circ\text{C}/\text{min}$, with a N_2 purge, up to 500°C . It is clear that the chitosan films have a thermal decomposition temperature (T_D) higher than 250°C . Due to its semirigid molecular backbone, chitosan does not show a glass transition before decomposition. Experimental data also demonstrated that al-

Table I Refractive Indices of Chitosan Thin Films Measured by Ellipsometry

Material	Chitosan/HAc	Chitosan/HAc-Er ³⁺	Chitosan/HAc-Nd ³⁺
Refractive index	1.500	1.503	1.504

though the thermal decomposition temperature is influenced by doping with rare-earth metal ions, all films survive to temperatures over 200°C. This temperature stability is beneficial in processes which require elevated temperatures.

The refractive index of the chitosan films was investigated by ellipsometry. The measured refractive indices are shown in Table I. All films exhibit a refractive index near 1.5, and no dependence on doping was observed. Across the wavelength range examined (from 300 to 700 nm), little dispersion was found.

One of the most important parameters in determining the usefulness of the material for waveguides in applications such as optical interconnects is the optical loss. There exist many experimental methods to determine the optical loss in a waveguide structure, including out-of-plane scattering, Fabry-Perot fringe contrast, and cut-back techniques.^{17,18} The two latter experiments require processing-intensive facet preparation and also result in the destruction

of the waveguide. In contrast, the out-of-plane scattering technique uses a prism to couple light into the waveguide requiring no special processing or complicated end-fire-coupling equipment. In addition, the technique is noninvasive, leaving the waveguide intact for further characterization.

A four-layer planar slab waveguide geometry was used in these experiments. The waveguide consists of a silicon wafer substrate, a silica (SiO₂) low refractive index buffer layer, the chitosan thin film waveguiding layer, and, finally, air. The SiO₂ lower cladding layer acted as a buffer to prevent any possible coupling of the guided wave into the absorbing substrate.

As described above, the loss measurement was made by measuring the scattered light emitted from the waveguide as a function of the position along the distance of the waveguide. Figure 4 is a typical room-temperature result of the waveguiding loss measurement of chitosan/HAc films at a wavelength of 830 nm taken at three different locations on the

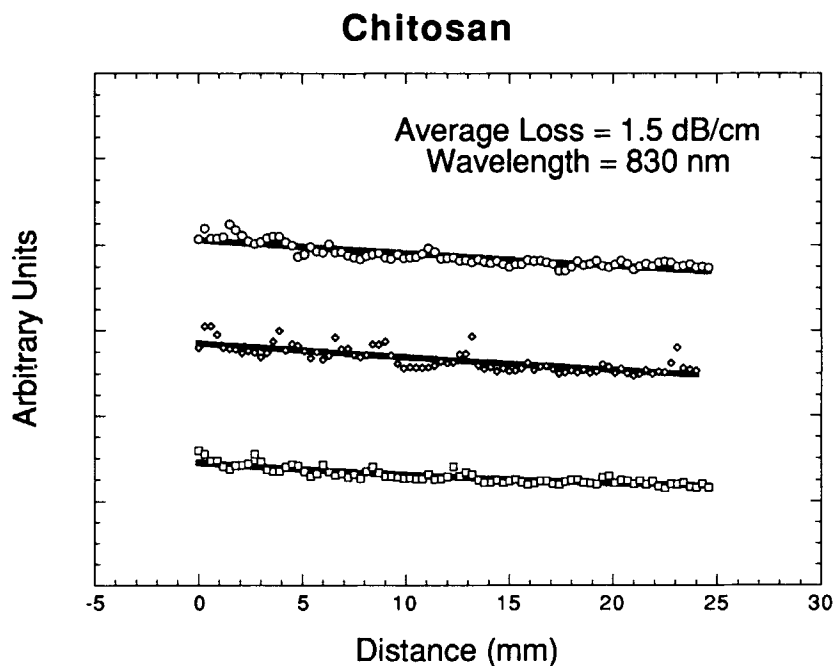


Figure 4 Examples of data obtained from the waveguiding loss measurements at 830 nm. The different sets of data represent measurements from three different areas of the same film. The line drawn through the data is a best fit and is used to calculate the average loss.

wafer. This wavelength was chosen because of its usefulness in short-haul communication systems, such as optical connects. The solid lines represent the least-squares fits to the data, in which the actual loss coefficient is extracted. Apparent noise in the experimental data was mostly attributed to scattering off large impurities or defects, such as dust, that was incorporated during film preparation. All three films, chitosan/HAc, and chitosan/HAc doped with Er^{3+} , or Nd^{3+} , exhibited nearly the same loss value of about 1.5 dB/cm with a measurement error of ± 0.1 dB/cm. Best values obtained were less than 0.5 dB/cm.

Generally, the main causes of propagation loss in straight waveguides are absorption and scattering. As seen in Figure 5, there is nearly no difference between the UV-vis spectra of all chitosan films (including the undoped and doped films which were

spin-coated onto glass substrates with a thickness of 1 micron) and that of the blank glass substrate. In other words, all the polymer films have a negligible optical absorption at room temperature over a wavelength range of 300–2700 nm. Combined with morphological characterization by LVHRSEM and TEM (which will be discussed later), it is reasonable to believe that scattering (and not absorption) losses were the dominating factor for the chitosan films.

Figures 6–8 are micrographs of the chitosan/HAc thin films measured with TEM and LVHRSEM. The surface morphology appears smooth and uniform (Fig. 7), and the structure is dense with few defects (Fig. 6 and Fig. 8, seen in cross section). Wide-angle X-ray diffraction and electron diffraction of all the chitosan films (with/without doping) also confirm an amorphous structure of these films and no clear evidence of forming crystallites was

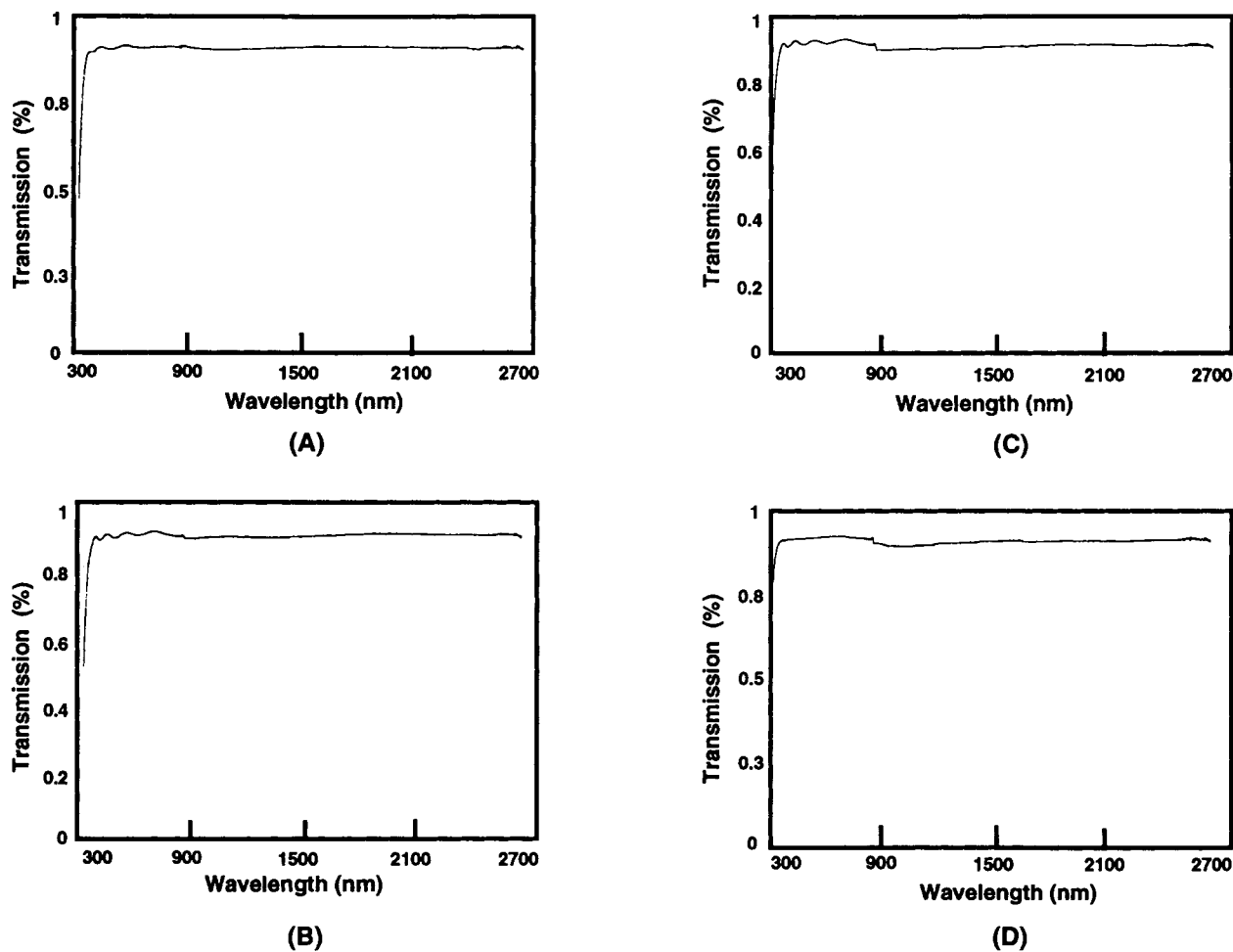
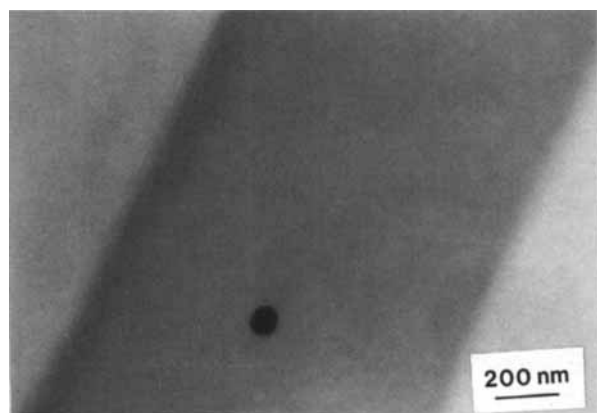


Figure 5 UV-vis spectra of various films (1 micron thick) from 300 to 2700 nm taken still attached to the glass substrates. (A) Chitosan, (B) chitosan doped with Nd, (C) chitosan doped with Er, and (D) the blank glass substrate spectra are shown.



(a)



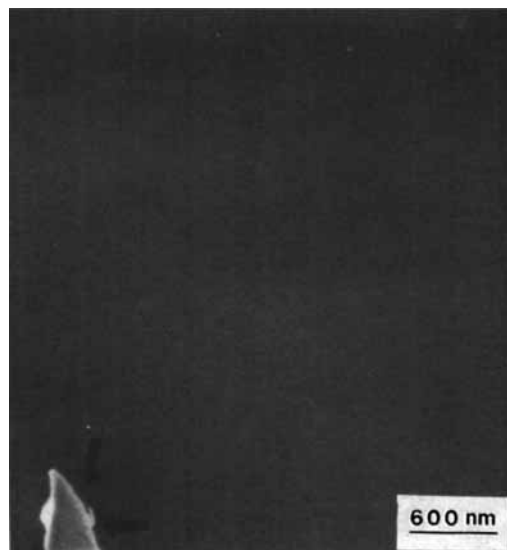
(b)

Figure 6 Typical TEM micrographs of ultramicrotomed films of chitosan-based materials obtained in the BF mode. Micrograph A shows a film with thickness approximately 1 micron. A small inclusion is shown in this micrograph. Both micrographs indicate a homogeneous bulk structure with few defects and particulates present.

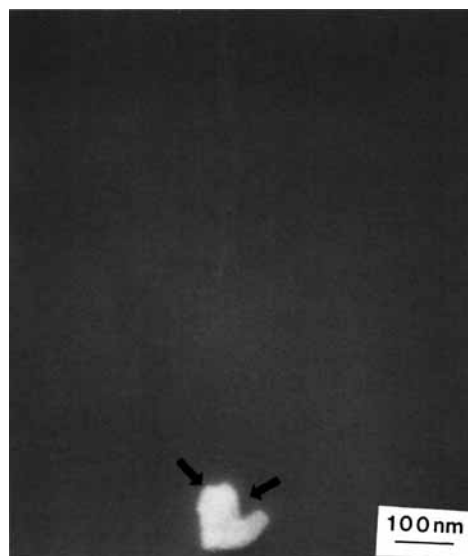
found. However, it is interesting to note from the WAXD pattern of the chitosan films that there exists a faint diffraction ring which might fit the characteristic diffraction of the anhydride crystals (at $2\theta = 20^\circ$, seen in Fig. 9). Crystallites in the films can cause scattering. It is possible that there might exist a small amount of crystallites in the chitosan films, which could come from two sources: One is the original anhydrous crystals in the raw materials, which are difficult to dissolve in acidic solvents^{19,20} and may remain in the final films, and the other is that some degree of aggregation of the rigid chitosan molecules could form in the dilute acetic acid solution.²¹ During processing, with the evaporation of solvents, the aggregation might act as the nuclei to form small crystallites.

AFM surface images (Fig. 10) support the conclusion of a homogeneous film structure. The RMS

roughness (measured with AFM surface images) of these films is less than 10 Å. Therefore, the low waveguide loss values could be attributed to the uniform and homogeneous amorphous structure of the films. In addition, the smoothness and low micro-

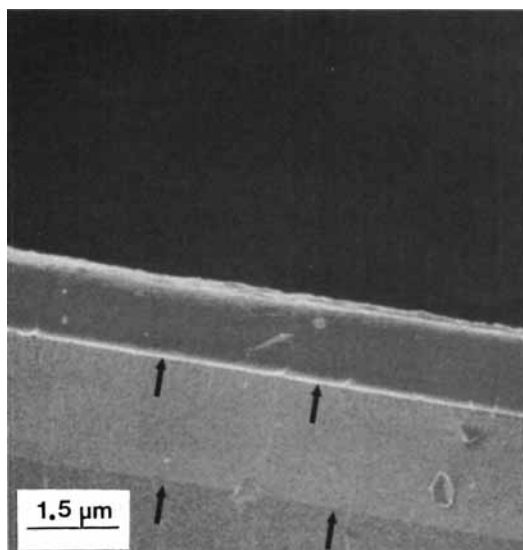


(a)

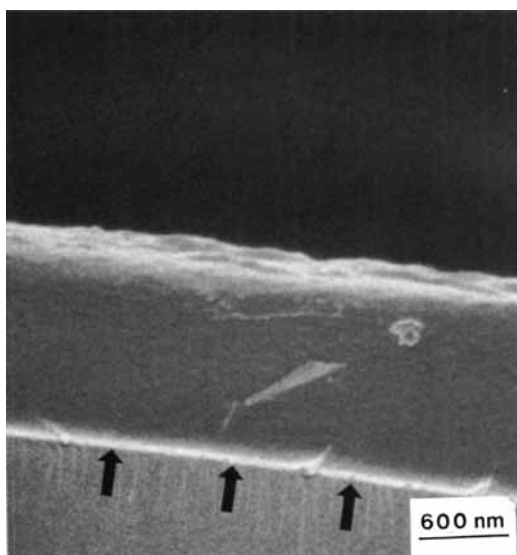


(b)

Figure 7 Characteristic LVHRSEM micrographs of the surface structure of chitosan-based thin films. Both indicate a smooth texture with the presence of a small number of particulates of various sizes as indicated by the arrows. It is these particulates that are thought to be the main cause of the extrinsic scattering loss observed.



(a)



(b)

Figure 8 Characteristic LVHRSEM micrographs of cross sections of chitosan-based thin films. Micrograph A shows the interface between the Si and the deposited SiO₂ and the interface between SiO₂ and the deposited chitosan thin film. The higher magnification micrographs show a clean fracture surface with few voids or particulates present.

roughness of the film surface also contribute to decreased optical scattering. All these facts imply that the intrinsic nature of chitosan films satisfies the requirements for a good waveguide material. The experimental results also suggest that extrinsic

scattering plays a key role in the optical losses of these films.

Extrinsic scattering is caused by impurities and imperfections. The waveguides were tested at different wavelengths (790, 830, and 950 nm) and the optical loss results were similar. It is well known that according to the Rayleigh and Mie theories scattering should be closely related to the wavelength.²² However, in our experimental range, there is no apparent differences in loss value. Therefore, it is reasonable to predict that the scattering loss is suggestive of loss by imperfections whose sizes are random and greater than the wavelength of the scattering light. These considerations combined with the TEM and LVHRSEM observations of homogeneous glassy films suggest that the surface impurities may be one of the determining factors affecting the loss values. During our experiments, it was easily seen that scattering by surface impurities when present, such as dust and particulate inclusions, caused serious optical losses during waveguiding. Also affecting these measurements was a nonuniform thin film thickness. Owing to problems in spin-coating processing and/or an initial uneven surface morphology of the substrates, some chitosan films were not uniform across the whole wafer. By means of a monochromatic green light source, it was observed that there were apparent variations in

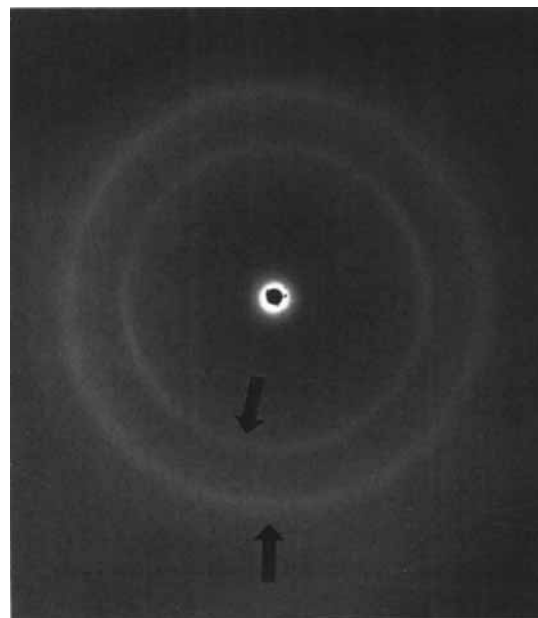


Figure 9 WAXD pattern from a chitosan-based thin films. Two faint, relatively diffuse rings are present as indicated by the arrows. Doping had little effect on these diffraction patterns.

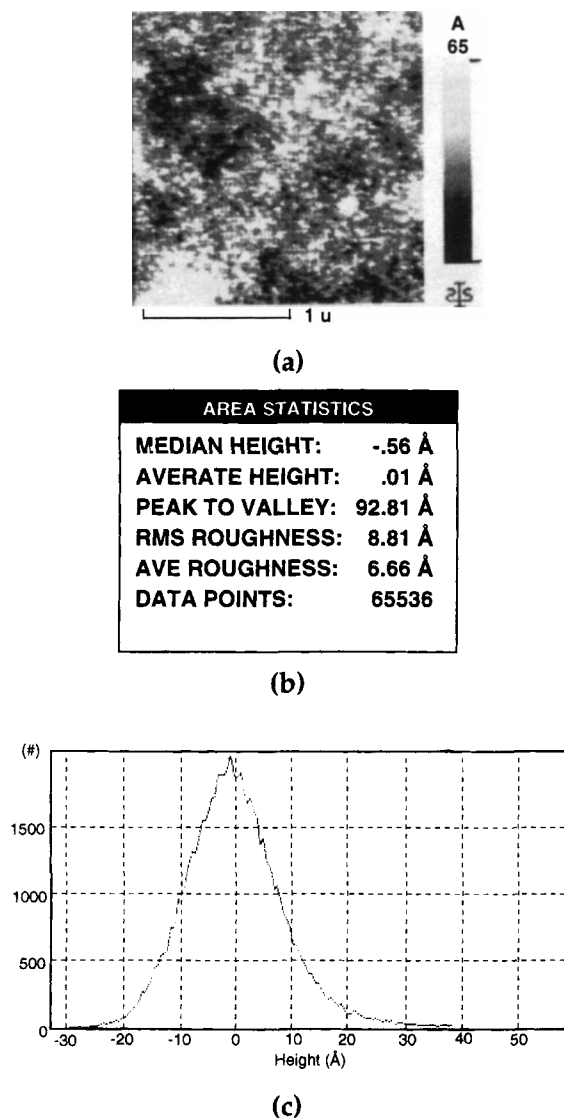


Figure 10 (a) AFM image of an approximately 1.5×1.5 micron region, (b) area statistics generated from the region revealing a low RMS roughness, and (c) the histogram of the median heights indicating a homogeneous (amorphous) distribution of roughness.

thickness of some films on the order of 500 Å. The difference in thickness between the edge and center led to variations in the waveguiding results, which clearly increased the optical loss due to guided light being coupled out of the surface of the waveguide.

Reduction of extrinsic scattering requires optimization of the film fabrication process. A series of experiments was performed to examine the influence of processing conditions on waveguiding loss. For the dissolving solution, the HAc concentration was kept in the range 0.5–10 wt % and preferably 1–3 wt %. Chitosan in the precursor solution was con-

trolled in the range of 0.5–5 wt %, preferably 1–3 wt %. Higher chitosan concentrations resulted in solutions with a too high viscosity which hindered purification of the precursor solution and led to an increase in optical loss. Compared to the films made with low molecular weight chitosan, the films made with medium molecular weight chitosan had higher optical loss (>2.5 dB/cm). This was related to light scattering in the precursor solution. The physical dimensions of the waveguides were also affected by the processing. Single-mode operation of the waveguide could be achieved in 1 micron-thick or less films, while multimode operation was observed in thicker guides, because of lower refractive index confinement. It is known that samples with poor adhesion between the tested film and the substrate will show poor waveguiding due to increased scattering. However, the fabrication of chitosan precursor solutions under clean conditions resulted in films with good adhesion properties. Therefore, it is reasonable to consider that the polymer-SiO₂ interface was not responsible for the optical loss.

It is interesting to note that all the films, whether made from the chitosan/HAc system or made from the systems of chitosan/HAc doped with Er³⁺ and Nd³⁺, show nearly the same losses in waveguiding, optical refractive indices, and similar morphological structures. It is known that chitosan has a limited capacity for doping with rare-earth metal ions.²³ Within the permitted range, increasing the doping amount of the rare-earth metal ions did not have a distinct effect on the measured optical loss and other properties, such as refractive index or morphological structure. When the doping ratio was increased over 40 wt %, the metal salts crystallized and precipitated out of the solution during the processing to form scattering sites in the films which degraded the optical quality of the waveguides.

CONCLUSIONS

Thin films made from a chitosan-dilute HAc solution show loss values of less than 0.5 dB/cm in a waveguide geometry. Films made from this material class are amorphous as shown by both WAXD and ED. TEM, LVHRSEM, and AFM observations indicate that these films have dense, uniform, and homogeneous bulk structures as well as smooth surfaces. The chitosan films also show good thermal stability and their decomposition temperatures are higher than 200°C. All these features indicate that chitosan is a potential candidate material for electrooptic applications. The experimental results also

imply that the extrinsic scattering caused by imperfections, particulate inclusions, and impurities (especially the surface impurities) and waveguide thickness uniformity were the main causes for the optical loss in our waveguide geometry.

It is interesting to note that for all three kinds of films, chitosan/HAc and chitosan/HAc doped with Er^{3+} or Nd^{3+} , their optical properties, including waveguide loss and refractive indices, and morphological characteristics are similar. This implies that in our experimental scale the basic molecular conformation in the chitosan films are not changed dramatically if chitosan forms complexes with rare-earth metal ions. More research is ongoing to understand the structure variations of the chitosan/HAc films with and without doping of the rare-earth ions in order to improve optical properties and to vary the refractive index of the films.

The authors thank sincerely Ms. Pamela Lloyd for her help in TEM work.

REFERENCES

1. M. J. Soileau, *SPIE Proceed.*, **1105**, 1 (1989).
2. P. N. Prasad and D. J. Williams, *Introduction to Nonlinear Optical Effects in Molecules & Polymers*, Wiley, New York, 1991.
3. B. L. Booth, *J. Lightwave Technol.*, **7**(10), 1445 (1989).
4. R. R. Krchnavek and D. L. Rode, *IEEE LEOS Newsl., Oct.*, 18 (1994).
5. B. Fan, D. G. Flagello, J. D. Gelorme, M. M. Oprysko, A. Speth, and J. M. Trewhella, Eur. Pat. Appl. 10446672A1 (1991).
6. R. Lytel, G. F. Lipscomb, E. S. Binkley, J. T. Kenney, and A. J. Ticknor, in *Materials for Nonlinear Optics: Chemical Perspectives*, Chap. 6, p. 103, 1991.
7. J. E. Midwinter and Y. L. Guo, *Optoelectronics and Lightwave Technology*, Wiley, Chichester, UK, 1992, p. 207.
8. W. J. Miniscalco, L. J. Andrews, S. Zemon, B. T. Hall, T. Wei, and R. C. Folweiler, in *MRS Symposium Proceedings*, **172**, 329 (1990).
9. H. Sucho, in *Guided Wave Nonlinear Optics*, D. Ostrowsky and R. Reinisch, Eds., Kluwer, Dordrecht, 1992, p. 187.
10. M. P. De Micheli, in *Optical Waveguide Materials, MRS Symposium Proceedings*, M. M. Broer, G. H. Sigel, Jr., R. Th. Kersten, and H. Kawazoe, **244**, 295 (1992).
11. R. T. Chen, *Opt. Laser Technol.*, **25**(6), 347 (1993).
12. S. Hirano, in *Chitin and Chitosan*, G. Skjak-braek, T. Anthonsen, and P. Sandford, Eds., Elsevier, London, 1989, p. 37.
13. P. A. Sandford, in *Chitin and Chitosan*, G. Skjak-braek, T. Anthonsen, and P. Sandford, Eds., Elsevier, London, 1989, p. 37.
14. H. Struszczyk, O. Kivekas, A. Niekraszewicz, and A. Urbanowski, *Text. Asia*, **7**, 80 (1993).
15. E. Kensky and D. Zelmon, *Rev. Sci. Instrum.*, **64**(7), 1794 (1993).
16. E. T. Kensky, *A Fully Automated Stage for Optical Waveguide Measurements*, WL-TR-93-4092 (1993).
17. M. Gottlieb, G. B. Brandt, and J. J. Conroy, *IEEE Trans Circuits Syst. CAS*, **26**, 1029 (1979).
18. R. G. Walker, *Electron. Lett.*, **21**, 581 (1985).
19. K. Ogawa, *Agric. Biol. Chem.*, **55**, 2375 (1991).
20. T. Yui, K. Imada, K. Okuyama, Y. Obata, K. Suzuki, and K. Ogawa, *Macromolecules*, **27**, 7601 (1994).
21. M. Rinaudo and A. Domard, in *Chitin and Chitosan*, G. Skjak-braek, T. Anthonsen, and P. Sandford, Eds., Elsevier, London, 1989, p. 71.
22. C. F. Bohren and D. R. Huffman, *Absorption and Scattering of Light by Small Particles*, Wiley, New York, 1983.
23. R. A. A. Muzzarelli, *Natural Chelating Polymers*, Pergamon Press, New York, 1973.

Received September 9, 1995

Accepted January 27, 1996